Submarine Canyon Architecture and Evolutionary in the Miocene Deepwater Taranaki Basin, New Zealand

Delvina Syaifira Norma Hani* and Piyaphong Chenrai

Petroleum Geoscience Program, Department of Geology, Faculty of Science,
Chulalongkorn University, Bangkok 10330, Thailand
*Corresponding author email: delvinasyaifira@gmail.com

Received: 12 Jun 2022
Revised: 19 Jul 2022
Accepted: 19 Jul 2022

Abstract

Despite the excessive cost of drilling operations and oil and gas instrumentation, the understanding of paleo-geometry has become crucial to lower the financial plan and maximize the drilling plans' performance. In offshore exploration, a three-dimensional seismic survey is critical for interpreting reservoir stratigraphy and depositional mechanisms, especially in the deeper marine basins. The submarine canyon in the deepwater Taranaki Basin has been modeled to have low sinuosity in the early channel system and higher sinuosity in the late channel system. The six main depositional architectures, such as basal lag (BL), erosional surfaces (ES), debris flows (DF), turbidite channels (TC), lateral accretion packages (LAPs), and mass transport deposit (MTD), were found in this canyon by seismic facies interpretation. High amplitude reflections (HARs) and Low amplitude reflections (LARs) that categorize those six-architecture elements can be used to identify the lithology in the individual channel. The channel evolution was recognized to occur in six-channel orders from the early Miocene channel system to the late Miocene channel system that influenced the channel stacking pattern types (lateral and vertical aggradation stacking patterns) in the study area. The depositional architecture and channel stacking pattern that creates channel complex systems were studied to consider reservoir connectivity and net-to-gross (N:G) ratio.

Keywords: submarine canyon, channel, sinuosity, architectures, evolution, stacking pattern.

1. Introduction

Submarine canyons are steep-sided, cut valley walls formed by erosional processes and mass wasting events on the continental shelf. Submarine canyon transfers sediment brought by the terrestrial river system from the continental shelf to the deepwater setting (Wonham et al., 2000; Bouma, 2001; Laursen and Normark, 2002; Popescua et al., 2004; Antobreh and Krastel, 2006; Harris and Whiteway, 2011; He et al., 2013). Many submarine canyons have been reported around the world, with varied geometry, stacking patterns, controlling factors, and canyon architecture (Deptuck et al., 2007; He et al., 2013; Zhou et al., 2015; We et al., 2018). Previous canyon studies have used 2D and 3D seismic data to examine canyon morphology, filling architecture, and controlling factors (e.g., Deptuck et al., 2007; Mayall et al., 2006; Li et al., 2013; He et al., 2013; Zhou et al., 2015; We et al., 2018). The complex architecture within each channel is the result of multiple internal erosion surfaces caused by the long-term evolution and interaction of channel erosion, aggradation, lateral migration, and levee deposition (Deptuck et al., 2003; Posamentier, 2003; Kane et al., 2009; Abreu et al., 2003; Mayall et al., 2006).

A growing number of studies have established channel migration as a critical process in the channel and canyon architecture (Wonham et al., 2000; Babonneau et al., 2002; Posamentier, 2003; Deptuck et al., 2007; McHargue et al., 2011). In addition, submarine canyon exploration is essential for petroleum target exploration of

hydrocarbon reservoirs in shallow to deep settings (Lastras et al., 2007; Wu et al., 2018).

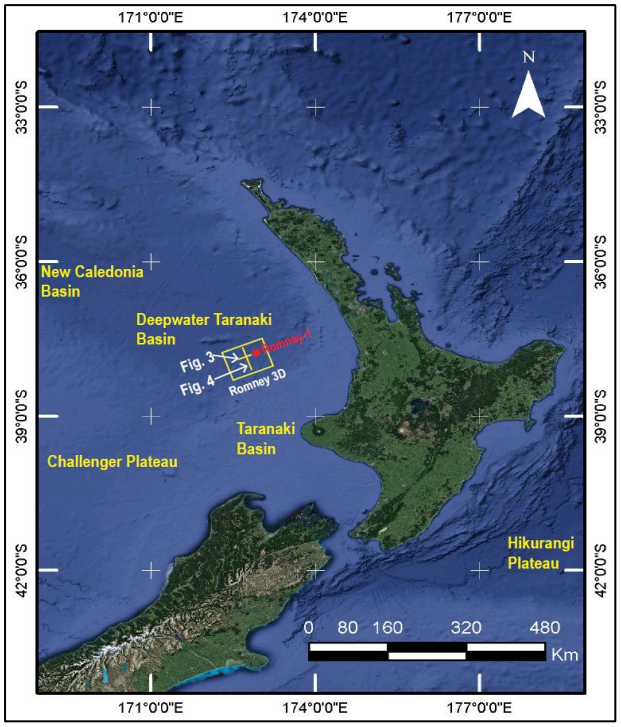

Figure 1 The study area is located within the Romney 3D survey (yellow rectangle). In addition, the Romney-1 well is available within the 3D seismic cube (red dot).

Submarine canyons transported mass and preserved a mass transport deposit within the canyon architecture, which was thought to be a mud-rich hydrocarbon trap (Moscardelli et al., 2006; Beaubouef and Abreu, 2010). Turbidite channels are commonly found in highly complex reservoir and lateral accretion package forms during migration, and these are estimated as an imported reservoir element in submarine channels system (Mayall et al., 2006). Turbidite channels, due to their diagenesis-controlled factors (slump, slides, debris flows, mud flows), can produce different individual channel patterns. This unique feature in the individual channel has been identified on the sinuosity, facies, cutting and filling episode, and channels stacking pattern (Mayall et al., 2006). Channel fills lithology has been grouped by Mayall and Stewart (2000) into basal lags, slumps, debris flow, high N:G stacked channels, and low net-to-gross (N:G) channel-levee facies elements. They were, furthermore, dividing the lithologies within the individual channels. The depositional architecture analysis can be helpful for rapid consideration to identify reservoir or non- reservoir facies, barriers, and baffles in terms of fluid accessibility (Mayall et al., 2006).

Shell Petrel acquired the earliest seismic data collection in 1969 in the Deepwater Taranaki Basin, when no wells had been drilled. Uruski and Wood (1991) were the pioneers who assessed petroleum prospects by studying single-channel and low-fold used seismic data. The presence of a thick sedimentary section was confirmed by the acquisition, processing, and interpretation of the basin's first modern multi-channel seismic line in 1997 (Uruski and Baillie, 2001). Therefore, Uruski (2008) used the DTB01-40 seismic line to examine the petroleum prospects within the Romney prospect and concluded that the mudstone-dominated interval in the Paleogene can be a great regional seal. On the other hand, the clastic sediment in the Miocene was produced by wide basin floor fans and channel system development located in the upper older Cretaceous structure. This paper aimed to assess the submarine canyon architecture and channel evolution within Romney 3D seismic survey area to suggest reservoir connectivity type in the deepwater Taranaki Basin (Figure 1). Moreover, understanding the reservoir type in the deepwater Taranaki Basin using seismic data may suggest effective and efficient further well planning.

2. Geological Setting

Deepwater Taranaki Basin, situated in the northwest extension of offshore Taranaki Basin, was formed as a Mesozoic rift basin by the evolution of the modern plate boundary through Zealandia from the Late Cretaceous to the Neogene (Schellart et al., 2006). Eastern and southern areas of the Taranaki Basin are located

within the active plate boundary deformation zone. However, western parts had remained relatively undeformed since the latest Paleocene (ca. 55 Ma), during which the Tasman Sea opening ceased and passive margin subsidence occurred (Gaina et al., 1998). During the Late Eocene to Early Miocene, the Taranaki Basin contracted in conjunction with the convergence of the Australian and Pacific plates (Strogen et al., 2014). This basin covered an area of 100,000 km^2 and contained a 10 km sedimentary section ranging from the Mid-Cretaceous to recent depositions (Stagpoole et al., 2001; Strogen et al., 2019).

Tectonic development from the early Cretaceous to early Eocene included the break-up of Gondwana and the rifting phase of the Tasman Sea (Grahame, 2015). The thrust belt development and uplift event in the study area significantly increased sedimentation in the deepwater Taranaki Basin during the early Miocene active margin compression (Holt and Stern, 1994). Throughout the early Miocene, terrestrial sedimentation was stored within the basin in the period of maximum transgression and uplift in the hinterland and was directed from the north to the east. Submarine fans were widespread in the middle Miocene and outgrew gradually from transgression to regression until the present day (King and Robinson, 1988). The Miocene succession is made up of thick Manganui Formation mudstone interbedded with Intra-Manganui sandstone (Figure 2). The great uplift event and paleoclimate in the study area contributed massive volume of sediments to the shelf and such volume was brought by the gravity flow to the deepwater Taranaki Basin (Grahame, 2015). The Neogene succession was dominated by enormous channels up to ten kilometers long and turbidity fans up to fifty kilometers long (Uruski, 2008).

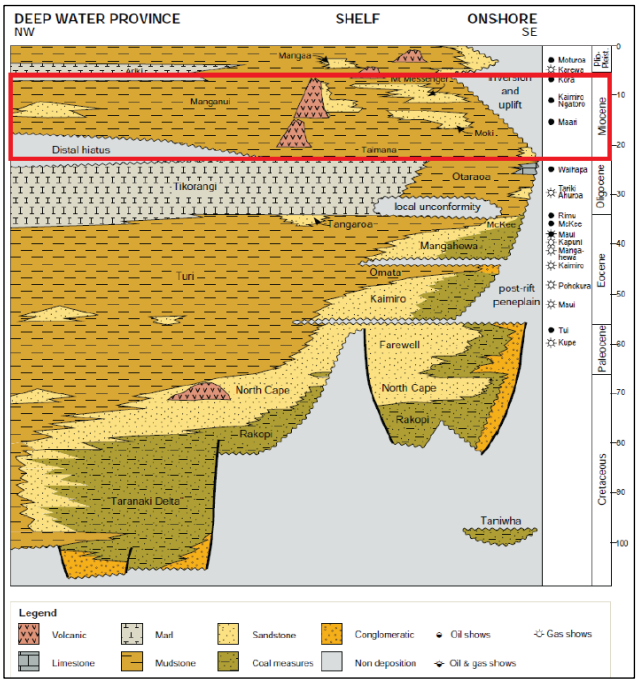

Figure 2 The stratigraphic chart of the deepwater Taranaki Basin. The focused interval is in the Miocene sediments (red square) (modified from Grahame, 2015).

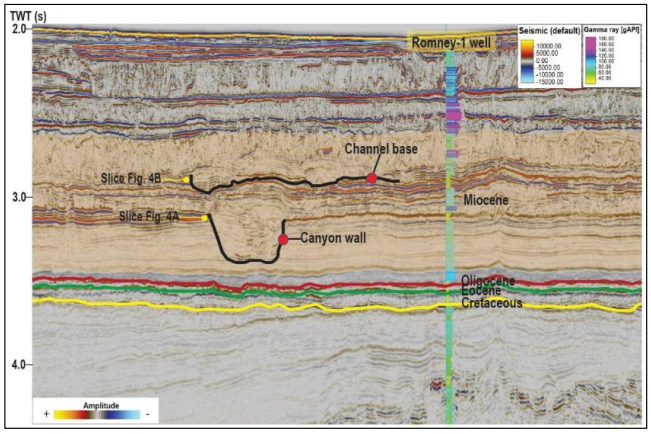

Figure 3 The seismic profile shows canyon and channel features within the Miocene successions. The geological ages presented as seismic horizon are from the Romney-1 well.

3. Data and Methodology

The primary data in this study came from the Romney 3D seismic survey acquired by Anadarko New Zealand in 2011 in the deepwater Taranaki Basin, approximately 150 km NW of the Taranaki Peninsula on the North Island. The Romney 3D was initially loaded into a Kingdom project before being imported into Petrel software. Romney-1 well was the sole well drilled inside the Romney 3D zone into 4,619 meters TVDSS (Total Vertical Depth Sub Sea). The gamma-ray log from Romney-1 well provided lithological information within this survey area (Figure 3). However, the Romney-1 well was placed outside the canyon bodies, which are the main target for this study.

Seismic attributes, such as original seismic, variance, and Root-Mean-Square (RMS), were generated using Petrel software to image canyon geomorphology and seismic facies types. The seismic attributes were used to delineate the individual channel depositional architecture, channel migration geometry, channel evolution, and canyon development.

4. Results

4.1 Channel Geometry

The submarine canyon in this study area was recorded within the Miocene deposition (Figure 3). The early Miocene channel system is 5 km wide and 30 km long. Likewise, the late Miocene channel system has around 2 km wide in the proximal and distal parts. This study observed that the flow direction of this canyon was from southeast to northwest direction. The canyon system occurred within the Manganui Formation and the formation is located at the depth of 2264 m to 2968 m TVDSS, according to well-seismic tie. The interpretation of channel geometry was conducted by seismic time-slice and cross-section to observe the channel's external geometry and channel preservation depth. The channel shape in this study area has been observed to be affected by repetitive change of channel migration. The amount of sediment brought by the stream channel was one of the controlling elements of bed change and, thus, channel migration. In addition, the flooding events can be another factor supporting the movement of sediment flux that influences the morphological adjustments of channels (Jarriel et al., 2021). The channel sinuosity is typically discussed as a result of channel migration processes in meandering channels (Lazarus et al., 2013). The channel has modifiable boundaries and a curved planform, implying to internal flow instabilities (Lazarus et al., 2013). Such flow instabilities drive spatial patterns of bank erosion and accretion, thereby altering the planform curvature (Lazarus et al., 2013). The sinuosity of the turbidite channels results from various processes, including erosion, lateral stacking, lateral accretion, and seafloor morphology (Mayall et al., 2006). Channel geometry has been studied and classified by the previous researchers (e.g., Schumm, 1985; Chruch, 1992; Brierley and Fryirs, 2004) and these studies support the argument in this research.

The channel geometry model has been pictured from the early Miocene channel system to the late Miocene channel system and they show a significant difference in geometry. The early channel system has been interpreted as an irregular meander type (Brierley and Fryirs, 2004, modified after Chruch, 1992). It obviously can be observed at the z-3128 seismic time-slice that the channel body shows a less-meandering channel (irregular meander type) (Figure 4A). The less-meandering geometry of this channel has low sinuosity in the range of 1,06 to 1,30 degrees of sinuosity based on Schumm (1985). This channel system has an average depth of 3.150 milliseconds Two-Way Time (ms TWT) and the deepest section was found in the distal area with depth of 3.350 ms TWT. On the other hand, the late Miocene channel system showed a distinct appearance from the older system. The late

Miocene channel system tends to have higher sinuosity of about 1,31 to 3,0 degrees and those values can be classified as a tortuous meanders channel type (Brierley and Fryirs, 2004 modified after Chruch, 1992) (Figure 4B). The average depth of this channel was recorded with the model at 2.950 ms TWT, shallower than the early Miocene channel system.

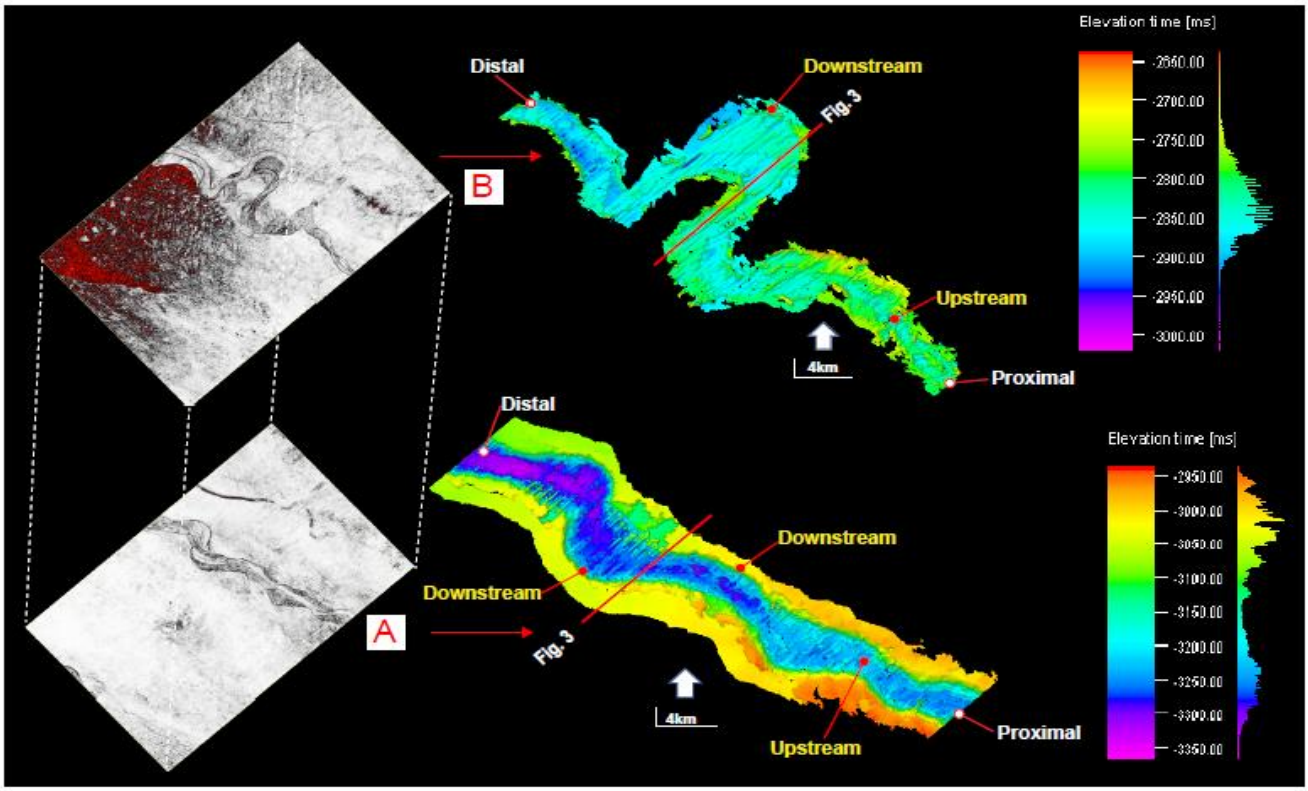

Figure 4 The model of channel geometry created from seismic cross-section and time slice in variance attribute that represents the channel meander and shift in the: A) early Miocene canyon and B) late Miocene channel.

4.2 Depositional Architecture

The seismic cross-section is used to interpret the depositional architecture characteristics. The classification is based on the seismic reflection and morphology in previous studies (e.g., Mayall et al., 2006; He et al., 2013; Wu et al., 2018). Submarine canyons in the deepwater Taranaki Basin have six main elements: mass transport deposit, basal lag, erosional surfaces, turbidite channel, debris flow, and lateral accretion packages (Table 1).

1. Mass transport Deposit (MTD)

Mass transport deposit is an essential element of the deepwater canyon system. This element in the study area is characterized by chaotic, weak to transparent amplitude reflection. Commonly, MTD preserves the uppermost basal lag and it is deposited in the center of the canyon (He et al., 2013). In this study area, this element is located primarily in the center part to the upper part of the canyon body. Mass transport deposits can be mud-prone sedimentary facies (Gong et al., 2010; He et al., 2013; Wu et al., 2018).

2. Base lag (BL)

Basal lag was identified as a thalweg deposit and it is a major element formed in the preliminary stages of individual canyon fill. Seismic facies of this architecture is reflected by high amplitude reflections (HARs), low

continuity, or even chaotic reflection. This element can be easily found on the base of the canyon body. Basal lag may have lithologies such as mud-clast conglomerate, coarse sand, and shale drapes deposited by the early canyon fill (Mayall et al., 2006; Wu et al., 2018).

3. Turbidite channel (TC)

The seismic facies for the turbidity channel were identified as chaotic, sheet-like geometry in high amplitude reflections (HARs). A single channel commonly occurs as a mounded-up (concave-up) seismic reflection. The erosional turbidite channel will appear in seismic reflection as convex-up geometry. In some locations, the turbidite channel in the study area has been recognized to occur in channel stacking patterns in lateral or vertical aggradation. The sandy turbidite channel is mainly reflected as the mounded-up geometry, while the concave-up geometry is identified as a muddy deposit (Wu et al., 2017).

Table 1 Canyon architectures observed in this study are divided into six elements; MTD: mass-transport deposit, BL; basal lag, TC: turbidite channel, ES: erosional surface, DF: debris flow, LAPs: lateral accretion packages.

Canyon Depositional Architecture	Seismic Images	Interpretation Drawing
1. Mass Transport Deposit (MTD) Sub-parallel or chaotic progradation with weak amplitude reflection.	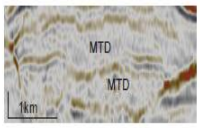	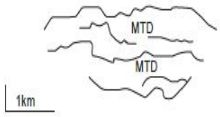
2. Basal Lag (BL) Chaotic, low continuity with high amplitude reflection.	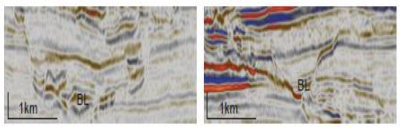	
3. Turbidite Channel (TC) Chaotic sheet-like geometry reflections, low to medium amplitudes like geometry. Concave-up geometry interpreted as muddy deposit. Convex-up/mounded facies represented as sandy sediment.	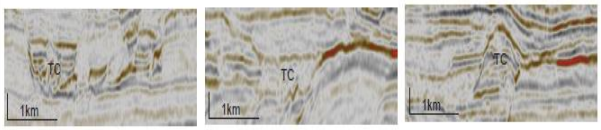	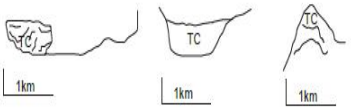
4. Erosional Surface (ES) High to medium reflection and high continuity with truncations seismic reflection.	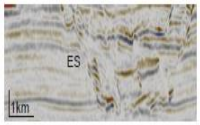	
5. Debris Flow (DF) On-lapping wavy or chaotic reflection, semi-transparent to low amplitude and low continuity.	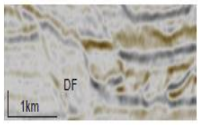	
6. Lateral Accretion Packages (LAPs) Sub-parallel, low continuity, medium to high amplitude reflection. Chaotic, low amplitude reflection and low continuity might occur in some point-bar.	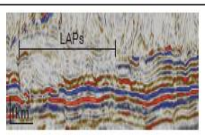	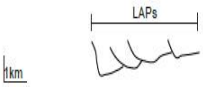

4. Erosional surface (ES)

A canyon wall of an erosional surface can generally be U- or V-shaped and this study area dominantly shows U-shaped. Erosional surface (ES) in the time slice is characterized by high amplitude reflection (HAR) and high continuity truncation reflection.

5. Debris flow (DF)

Debris flow was described by chaotic or onlapping, wavy reflection and semi-transparent to low amplitude reflection in low continuity. This element reflected the canyon fill stage that deposited muddy matrix or even muddy sand within the individual channel architecture (e.g., Mayall et al., 2006; Li et al., 2017). In this study, debris flow commonly occurs in the western and eastern part of canyon fill deposited in the upper part of basal lags seismic facies.

6. Lateral accretion packages (LAPs)

The LAPs were identified in the seismic profile by sub-parallel, high continuity in the medium to high amplitude reflection. The LAPs were also characterized by chaotic reflection with dominantly medium amplitude at the top and thin high amplitude at the base of the channel. Previous researchers have identified the lateral accretion packages as sandy deposits (e.g., Posamentier, 2004; He et al., 2013); however, this element may also be characterized by mud-prone deposits.

4.3 Channel Evolution

The canyon evolution was observed to grow as a new channel system in the upper part of the channel (Figure 3). This section will discuss the canyon system as the 'early Miocene channel system' and the younger channel as the 'late Miocene channel system'.

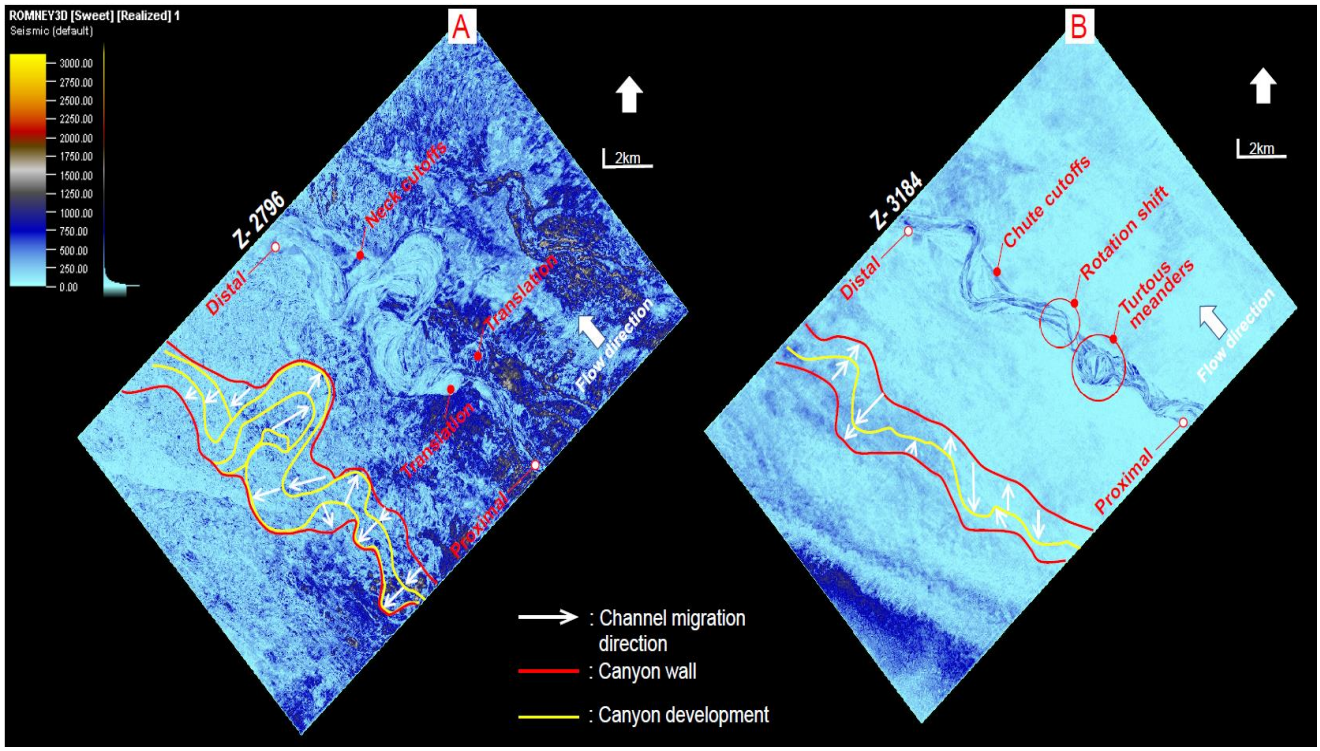

Figure 5 The RMS time slices of A) late Miocene channel system and B) early Miocene canyon. The white arrows point the direction of each channel's development migrating from the first to final stage by-product of channel stacking pattern.

The early Miocene channel system was identified as a semi-organized stacking pattern in which the channel migrated over time but in the same direction (Figure 5A). First, the channel system showed symmetrical migration in narrow-shaped channels with dominant downstream migration during the first channel distribution. Then, the channel system gradually broadens to an extensive channel in the second order channel. The last channel order in this canyon system changed to a minor meander than the previous older channel with extreme looping (orange line in Figure 6). Nonetheless, the channel sinuousity decreased and a significant upstream formed, specifically in the parallel direction with the flow direction. Moreover, the occurrence of chute cutoff in the RMS seismic time slice represents a decrease in stream length or sinuosity of the channel (Figure 5B).

The late Miocene channel system shows an organized stacking pattern, where the individual channel order has a unidirectional migration pattern (Figure 5B). The individual channel consistently transformed laterally into a narrow shape. Unlike the early Miocene channel system, this channel system has a high degree of sinuosity and a lateral stacking pattern. In this channel system, cutoff morphology was identified as neck cutoff or oxbow, specifically in the distal part (Figure 7). The deposition of the neck cutoff is similar to that of the chute cutoff, and the abandoned channel may be filled with finer sediments. Most of the channel translation or downstream progress is found on the left side of the channel.

4.4 Canyon Development

The Deepwater Taranaki Basin submarine canyon evolved in six stages. Time slice z-3128 (orange line) depicts the first channel development (Figure 6A). In time slice z-3176 (pink line), the second channel developed far-end from the first stage and built an extreme channel loop (Figure 6A). The third channel segment (green line) migrated similarly to the second channel but with lesser bending (Figure 6A). Channel migration contributed significantly to the formation of canyon or channel architecture (Deptuck et al., 2007).

In cross-section, the proximal canyon (IL 1050) produced a channel with a lateral aggradation stacking pattern (Figure 7B). Basal lag formed as a result of first-stage canyon erosion. Turbidite channel and mass transport deposit facies appeared laterally above the aggrading stacked channel. Debris flow occurred on the canyon walls and was commonly seen on the basal lag due to canyon erosion (e.g., Zhou et al., 2015). The canyon architecture preserved the lateral migration stacking pattern indicated by lateral accretion packages in the middle.

The second order channel migrated to the west after the first channel developed, resulting in vertical aggradation. The stacking pattern changed to lateral migration in the middle of the canyon, as evidenced by the third channel's movement. The architecture inside the canyon in the distal part is relatively consistent compared to the middle part. However, high-amplitude reflections were obtained in the upper and middle of the canyon body observed in the distal of the canyon (Figure 6B).

In the upper part of the canyon body, the late Miocene channel system developed with a multiple-meander channel complex. The late Miocene channel appeared more expansive than the canyon below. This channel's development is divided into three stages based on time slices in Figure 7A. First, from the previous channel (red line; 4th order channel), the 5th order channel (blue line) moved to the center of the channel body. Next, Channel 6th (yellow line) migrated laterally to the west crossing over channel order 4th.

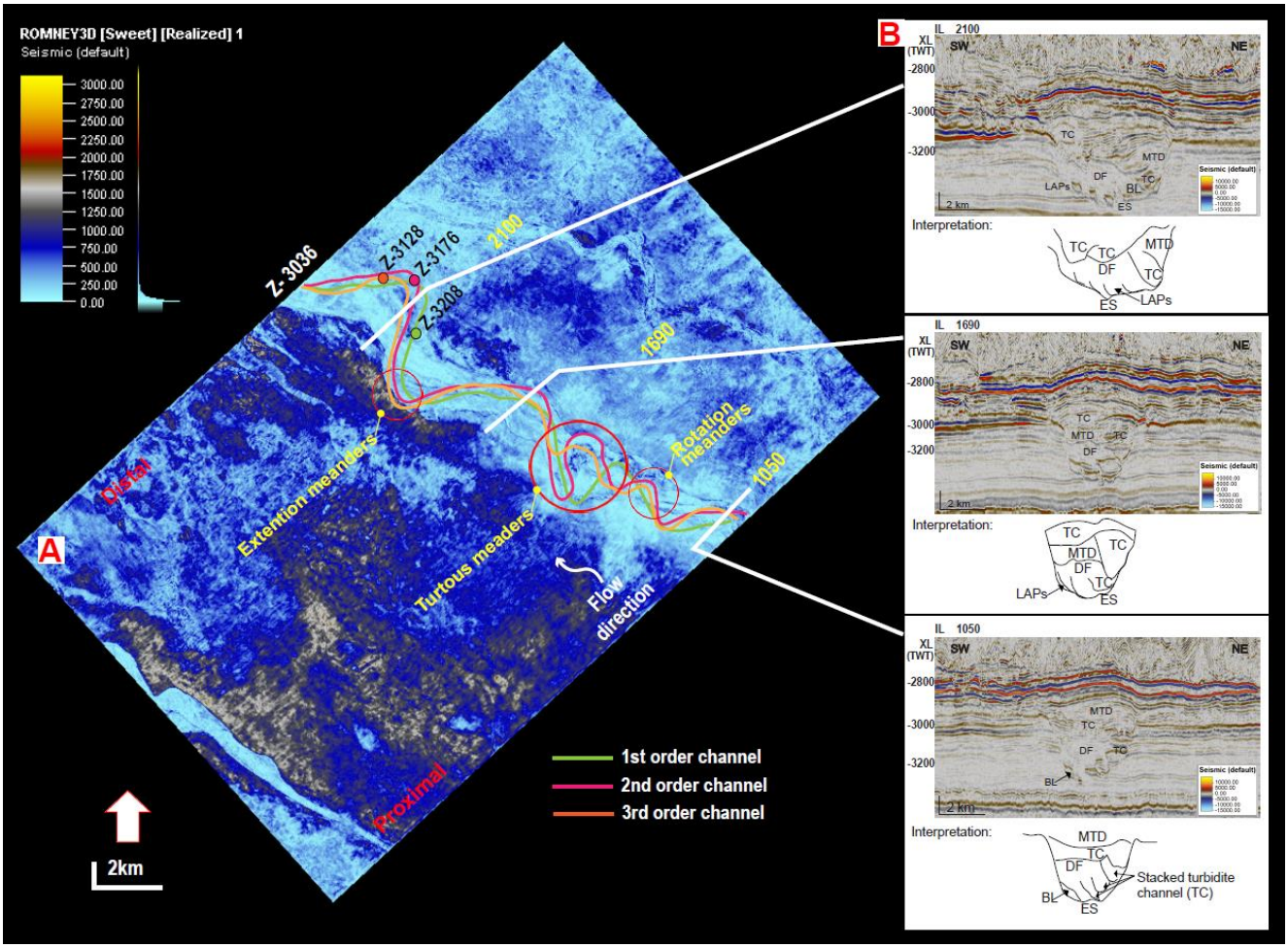

Figure 6 A) The illustration of a canyon development in the early Miocene channel system traced by seismic time slice in RMS attribute B) The interpretation of channel architecture described by seismic cross-section showing difference architecture from the proximal to distal area.

The channel architecture from IL 1050 seismic profile in the proximal part shows lateral accretion packages that can be defined as a point-bar. The basal lag in the channel was identified as a thalweg deposit (Figure 7B). The lateral accretion packages deposited on the left side of IL 1690 (Figure 7A) may be the result of channel order 6th. The channel on the right side could be the outer side of channels order 4th and 5th.

The channel architecture in the distal part is complex due to low sinuosity and downstream stacking pattern (IL 1940; Figure 7B). Although the lateral accretion packages in the IL 1940 were observed in the opposite direction, the deposit of channel order 6th (yellow line; Figure 7A) changed the meander direction. Furthermore, the parallel convex-up geometry with weak amplitude reflection was interpreted as the channel 6th's outer bank. The channels 4th and 5th in this section were challenging to identify and they are assumed to be eroded by the younger channel development.

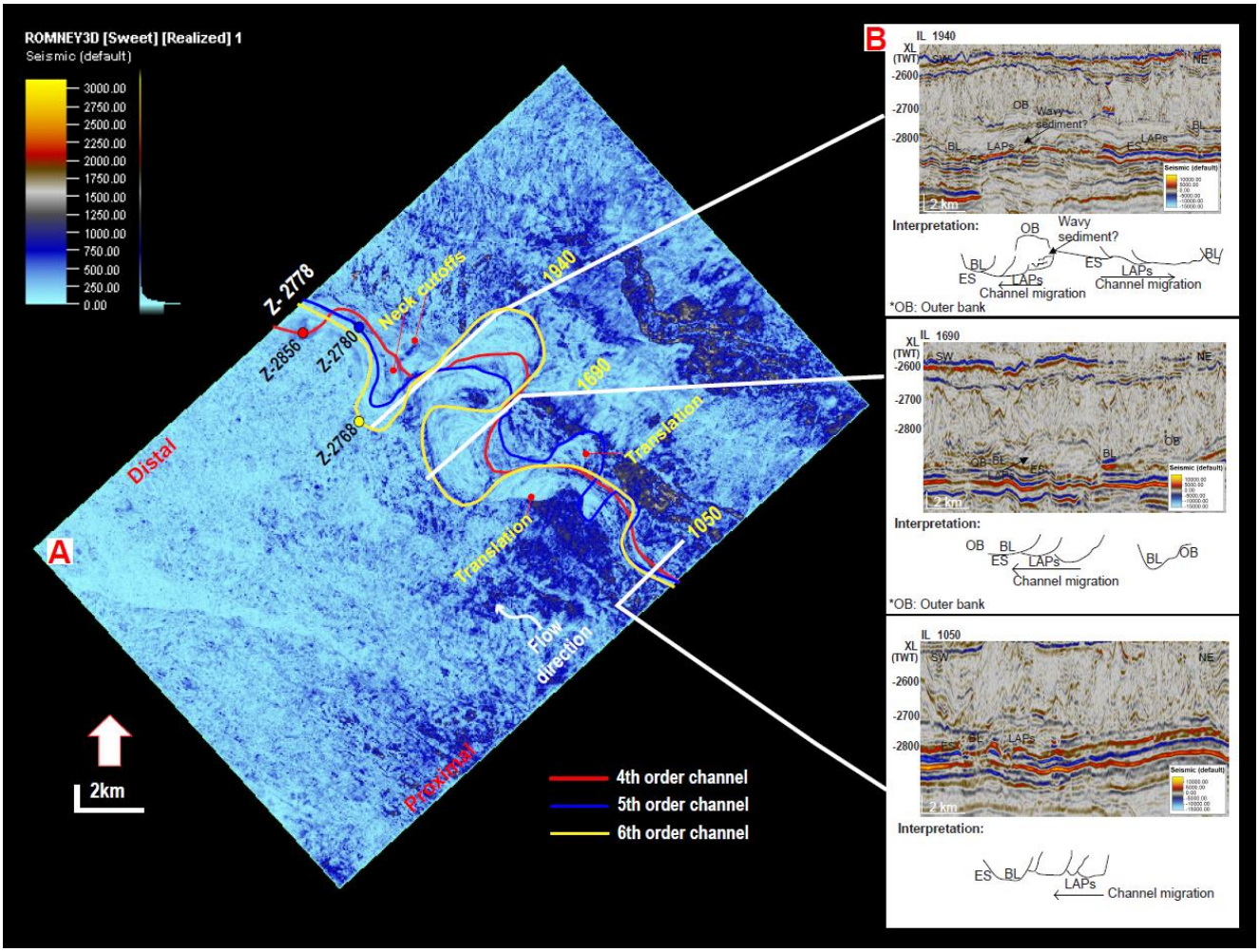

Figure 7 A) The illustration of a canyon development in the late Miocene channel system traced by seismic time slice in RMS attribute B) The interpretation of channel architecture described by seismic cross-section showing difference architecture from the proximal to distal area.

5. Discussion

5.1 Channel Deposition

Canyon deposition has been modeled using seismic cross-section and map view to understand the depositional architecture and to track the channel evolution. The deposition stage is divided into six units ranging from the early Miocene (DS1-DS3) to the late Miocene (DS4-DS6) of the Manganui Formation. The lithofacies described in this channel complex correspond to the amplitude reflections, with high amplitude reflection (HARs) interpreted as a sand body and muddy deposits identified in low amplitude reflection (LARs).

5.1.1 Deposition Stage 1 (DS1)

The first stage of canyon deposition is characterized by debris flow and basal lags. The DS1 cut and fill events were aided by erosion and turbidity currents along the first-order channel (Figure 6A; green line). Basal lag deposits are formed during canyon cutting and are composed of coarse sediment, mud-clast conglomerate, and shale drapes a few meters thick (Mayall et al., 2006) (Figure 8). Debris flow deposits are mud-prone sediments,

particularly in chaotic seismic facies (Posamentier and Kolla, 2003).

The depositional architecture of this unit indicates an erosional-deposit stage (e.g., He et al., 2013). Therefore, turbidite channel and basal lag reservoirs should be considered as prospective reservoirs with medium net-to-gross (N:G) (Mayall et al., 2006). Furthermore, the debris flow deposits can function as an effective seal (Figure 9).

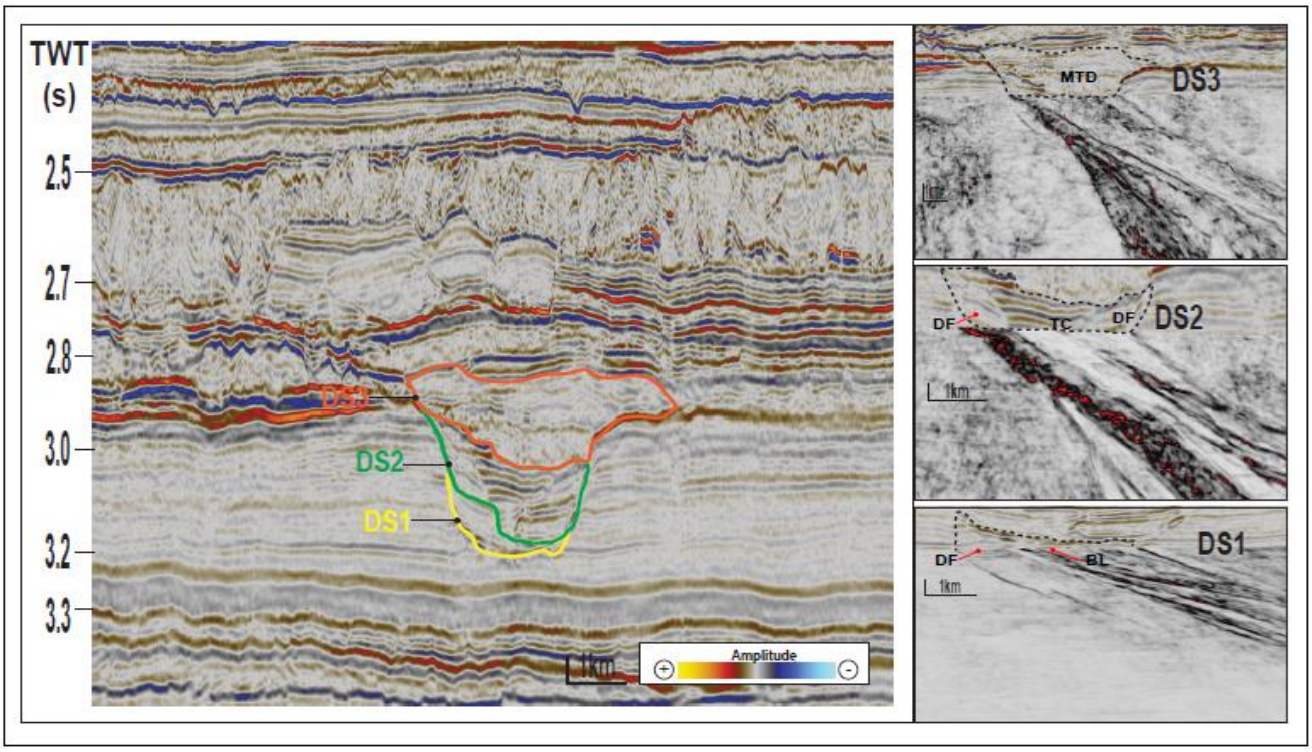

Figure 8 The depositional architecture and channel evolution inside DS1 to DS 3 were interpreted from seismic cross-section and variance seismic attributes.

5.1.2 Deposition Stage 2 (DS2)

The sandy turbidite channels are vertically-stacked in this unit as aggrading sequences (Figure 7B). The debris flow deposits occur in the southwest and northeast of this stage. The turbidite channel in DS2 eroded the first channel directly and wiped the mud drapes (Figure 8).

The incision deposit in the DS1 indicates that the DS2 was a smaller channel that eroded and removed the substantial sediment in the DS1 (Mayall et al., 2006). The model (Figures 9A-C) represented sand amalgamations with a vertical aggradation stacking pattern classified as high N:G (Mayall et al., 2006). The proximal part of this unit may not have good connectivity in a channel stacking pattern but has a good volume of sandy deposits (Figure 9D).

5.1.3 Deposition Stage 3 (DS3)

The DS3 deposit contains a massive mass transport deposit (Figure 8). Therefore, the high amplitude reflection may indicate the outer levee rather than the turbidite channel. In addition, a bypass channel occurs with low amplitude in the southwest point of the canyon.

However, the mud drapes covering the upper part of the sandy body from MTD may become a trap element (Figure 9).

5.1.4 Deposition Stage 4 (DS4)

DS4 is located on the top of the differential compaction layers (built-up reflections) and in the upper part of the canyon bodies (DS1-DS3). The lateral accretion packages in weak amplitude reflections dominate the depositional architecture in this unit (Figure 10). The lateral migration (swing pattern) produced DS4 and was recognized as a bypass deposit. However, the LAPs reflected in medium weak amplitudes along the channel body are interpreted as unstable LAPs merged with MTD (He et al., 2013). This channel was also identified as a mud-prone deposit (Figure 11). A large number of mud-prone layers can act as an excellent sealing element.

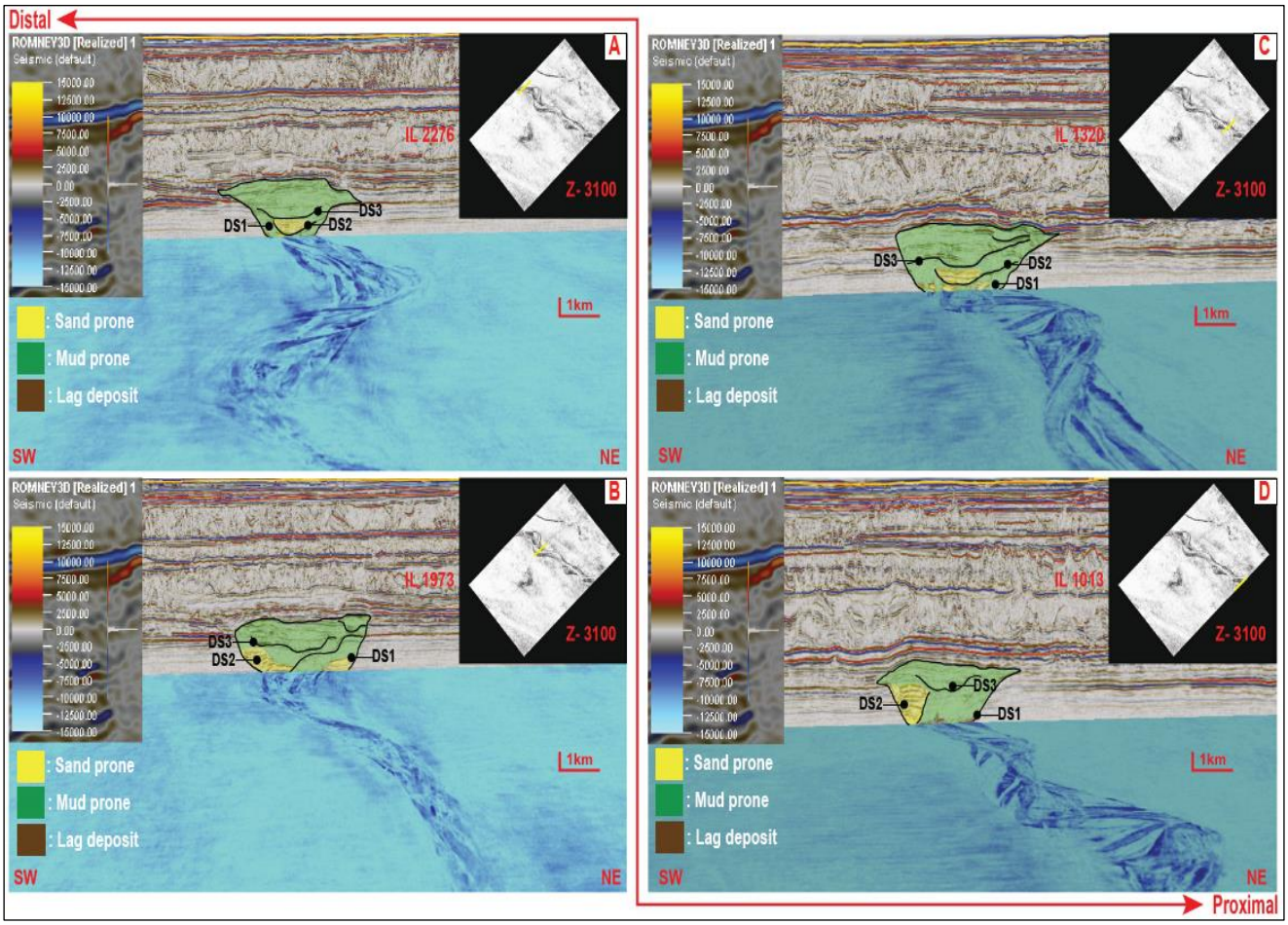

Figure 9 The interpretation of channel development DS1-DS3 from the distal to proximal parts.

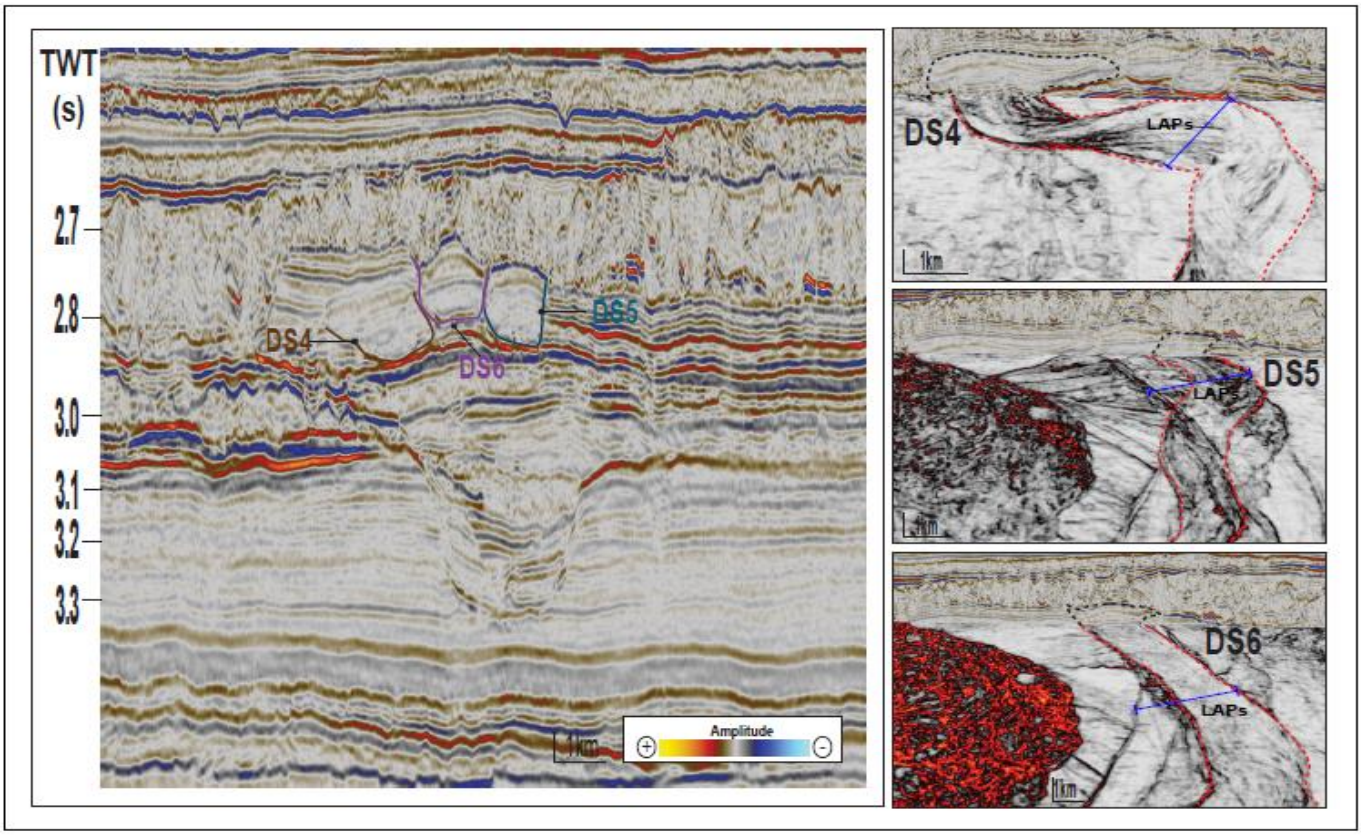

Figure 10 The interpretation of seismic cross-section and variance seismic attributes illustrated the architecture and channel evolution from DS4 to DS6.

5.1.5 Deposition Stage 5 (DS5)

The second stage of channel deposition (DS5) in this unit is composed of sub-parallel lateral accretion packages with low amplitude reflections and basal lag with high amplitude reflections. Large lateral stacking pattern due to channel migration produced DS5 (Figure 10). Basal lag deposition can be indicated by coarse sediments in the channel's thalweg. Conversely, this channel deposition can be a preferable reservoir in low net-to-gross (N:G) (Mayall et al., 2006) (Figure 11).

5.1.6 Deposition Stage 6 (DS6)

Deposition stage 6 is the final deposition and has a wider swing stacking pattern from channel migration than the previous units (Figure 10). Revealed by high amplitude reflections, this unit is made up of lateral accretion packages and basal lag and is classified as a thalweg deposit (Figure 11).

The sandy body identified by the presence of basal lag in the DS6 could become a possible reservoir in low net-to-gross (N:G) conditions (Mayall et al., 2006). The mud drapes that form on top of the sandy body can also serve as a suitable seal segment.

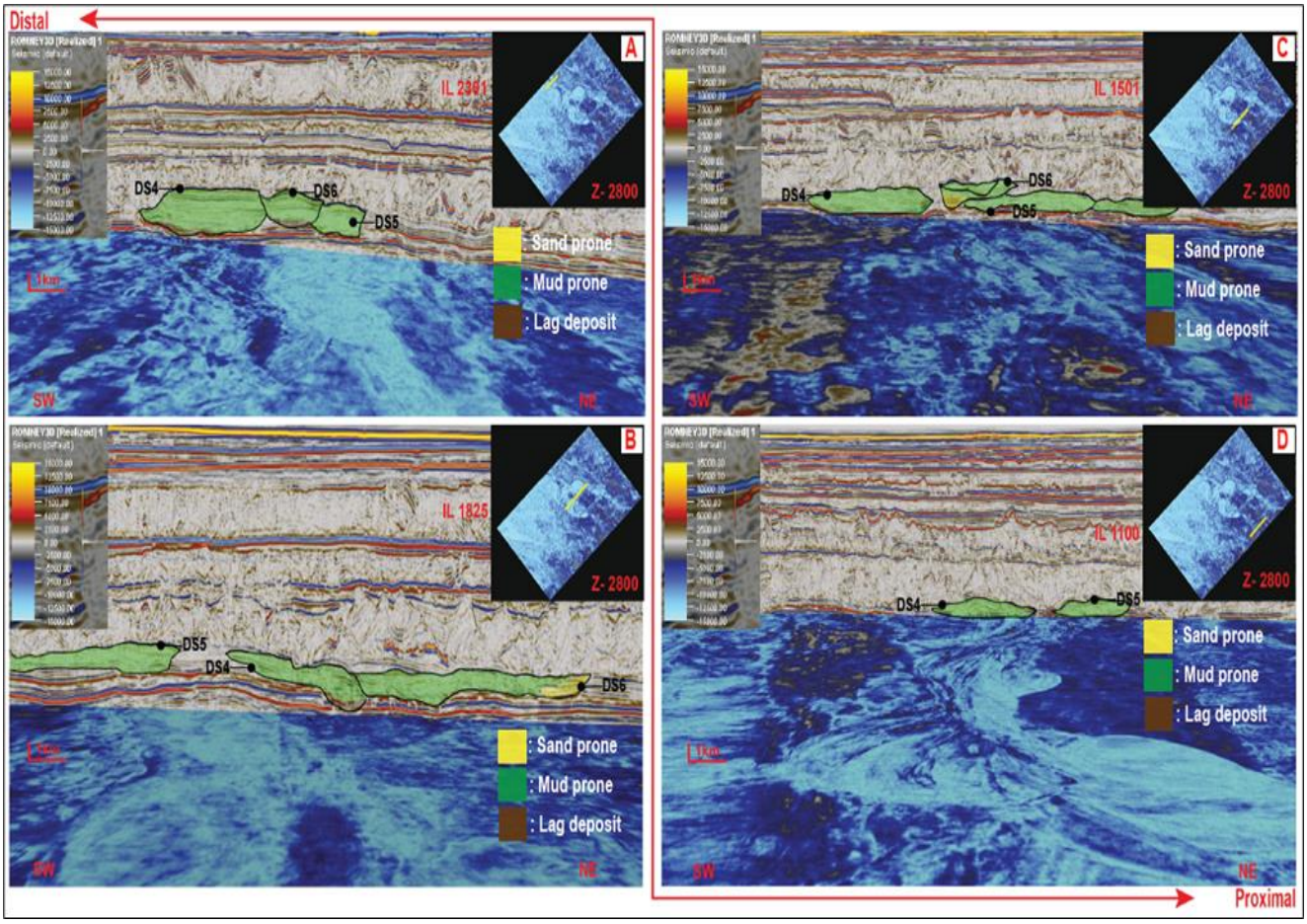

Figure 11 Channel depositions and stacking patterns from DS4-DS6 in the late Miocene channel system.

6. Conclusions

The study of depositional architecture, channel geometry, channel evolution, canyon development, and channel deposition of a submarine canyon in the deepwater Taranaki Basin can be summarized in the following points based on seismic interpretation from the 3D Romney survey:

1. The channel geometry model illustrated that the sinuosity of the early Miocene channel system was described as irregular meander (passive meander) with low sinuosity (1.06 to 1.30 degrees). On the other hand, the late Miocene channel was identified as tortuous meanders with greater sinuosity (1.31-3.0 degrees).

2. In the deepwater Taranaki Basin, six depositional architecture elements have been observed within the canyons: erosional surface (ES), turbidite channel (TC), debris flow (DF), lateral accretion packages (LAPs), mass transport deposit (MTD) and basal lag (BL).

3. The early Miocene channel system was created by a semi-organized stacking pattern. The late Miocene channel system was discovered to be an organized stacking pattern with a high lateral migration process. Oxbows can be seen in this channel system as a result of meandering growth evolution caused by neck cutoffs.

4. Canyon development in this submarine canyon grows six times at various development

stages. The channel order from 1 to 3 (Figure 6) were deposited inside the canyon body, while the 4th to 6th order channel) (Figure 7) were preserved in the topmost of the canyon as a fluvial channel. The early Miocene channel system is a preferable reservoir target with medium to high N:G and is possible an excellent sealing element. Otherwise, the late Miocene channel system is preferable to become sealing element due to low chance of course sediment consisted in the individual channel.

Acknowledgments

The first author acknowledges the generous financial support from Talented Petroleum Geoscientist Scholarship for offering financial aid during master's degree at Chulalongkorn University.

References

Abreu, V., Sullivan, M., Pirmez, C., & Mohrig, D. 2003. Lateral accretion packages (LAPs): an important reservoir element in deep water sinuous channels. Marine and Petroleum Geology, 20(6-8), 631-648.

Antobreh, A. A., & Krastel, S. 2006. Morphology, seismic characteristics and development of Cap Timiris Canyon, offshore Mauritania: a newly discovered canyon preserved-off a major arid climatic region. Marine and petroleum geology, 23(1), 37-59.

Babonneau, N., Savoye, B., Cremer, M., & Klein, B. 2002. Morphology and architecture of the present canyon and channel system of the Zaire deep-sea fan. Marine and Petroleum Geology, 19(4), 445-467.

Beaubouef, R. T., & Abreu, V. 2010. MTCs of the Brazos-Trinity slope system; thoughts on the sequence stratigraphy of MTCs and their possible roles in shaping hydrocarbon traps. In Submarine mass movements and their consequences (pp. 475-490). Springer, Dordrecht.

Bouma A H. 2001. Fine-grained submarine fans as possible recorders of long- and short-term climatic changes. Global and Planetary Change, 28: 85-91.

Brierley, G.J. and Fryirs, K.A., 2013. Geomorphology and river management: applications of the river styles framework. John Wiley and Sons.

Church, M., 1992. Channel Morphology and Topology. In:TheRivers Handbook, C. Calow and G. Petts (Editors). Blackwell,Oxford, United Kingdom, 2:126-143.

Deptuck, M. E., Steffens, G. S., Barton, M., & Pirmez, C. 2003. Architecture and evolution of upper fan channel-belts on the Niger Delta slope and in the Arabian Sea. Marine and Petroleum Geology, 20(6-8), 649-676.

Deptuck, M.E., Sylvester, Z., Pirmez, C. and O'Byrne, C., 2007. Migration–aggradation history and 3-D seismic geomorphology of submarine channels in the Pleistocene Benin-major Canyon, western Niger Delta slope. Marine and Petroleum Geology, 24(6-9), pp.406-433.

Grahame, J.L. 2015. Deepwater Taranaki Basin, New Zealand—New Interpretation and Modelling Results for Large Scale Neogene Channel and Fan Systems: Implications for Hydrocarbon Prospectivity.

Harris, P. T., & Whiteway, T. 2011. Global distribution of large submarine canyons: Geomorphic differences between active and passive continental margins. Marine Geology, 285(1-4), 69-86.

He, Y., Xie, X., Kneller, B. C., Wang, Z., & Li, X. 2013. Architecture and controlling factors of canyon fills on the shelf margin in the Qiongdongnan Basin, northern South China Sea. Marine and Petroleum Geology, 41, 264-276.

Holt, W. E., & Stern, T. A. 1994. Subduction, platform subsidence, and foreland thrust loading: The late Tertiary development of Taranaki Basin, New Zealand. Tectonics, 13(5), 1068-1092.

Kane, I. A., Dykstra, M. L., Kneller, B. C., Tremblay, S., & McCAFFREY, W. D. 2009. Architecture of a coarse-grained channel–levée system: the Rosario Formation, Baja California, Mexico. Sedimentology, 56(7), 2207-2234.

King, P. R., & Robinson, P. H. 1988. An overview of Taranaki region geology, New Zealand. Energy exploration & exploitation, 6(3), 213-232.

Kolla, V. and Posamentier, Henry and Wood, Lesli. 2007. Deep-water and fluvial sinuous channels—Characteristics, similarities and dissimilarities, and modes of formation. Marine and Petroleum Geology. 24. 388-405. 10.1016/j.marpetgeo.2007.01.007.

Lastras, G., Canals, M., Urgeles, R., Amblas, D., Ivanov, M., Droz, L., & García-García, A. 2007. A walk down the Cap de Creus canyon, Northwestern Mediterranean Sea: Recent processes inferred from morphology and sediment bedforms. Marine Geology, 246(2-4), 176-192.

Laursen, J., & Normark, W. R. 2002. Late Quaternary evolution of the San Antonio Submarine Canyon in the central Chile forearc (~ 33 S). Marine Geology, 188(3-4), 365-390.

Li, X., Fairweather, L., Wu, S., Ren, J., Zhang, H., Quan, X., & Wang, D. 2013. Morphology, sedimentary features and evolution of a large palaeo submarine canyon in Qiongdongnan basin, Northern South China Sea. Journal of Asian Earth Sciences, 62, 685-696.

Mayall, M., & Stewart, I. 2000. The architecture of turbidite slope channels.

Mayall, M., Jones, E., & Casey, M. 2006. Turbidite channel reservoirs—Key elements in facies prediction and effective development. Marine and Petroleum Geology, 23(8), 821-841.

McHargue, T., Pyrcz, M. J., Sullivan, M. D., Clark, J. D., Fildani, A., Romans, B. W., & Drinkwater, N. J. 2011. Architecture of turbidite channel systems on the continental slope: patterns and predictions. Marine and petroleum geology, 28(3), 728-743.

Moscardelli, L., Wood, L., & Mann, P. 2006. Mass-transport complexes and associated processes in the offshore area of Trinidad and Venezuela. AAPG bulletin, 90(7), 1059-1088.

Popescu, I., Lericolais, G., Panin, N., Normand, A., Dinu, C., & Le Drezen, E. 2004. The Danube submarine canyon (Black Sea): morphology and sedimentary processes. Marine Geology, 206(1-4), 249-265.

Posamentier, H. W., & Kolla, V. 2003. Seismic geomorphology and stratigraphy of depositional elements in deep-water settings. Journal of sedimentary research, 73(3), 367-388.

Posamentier, H.W. 2005. Application of 3D seismic visualization techniques for seismic stratigraphy, seismic geomorphology, and depositional systems analysis: Examples from fluvial to deep-

marine depositional systems analysis: Examples from fluvial to deep-marine depositional environments. 10.1144/0061565.

Schellart, W. P., Lister, G. S., & Toy, V. G. 2006. A Late Cretaceous and Cenozoic reconstruction of the Southwest Pacific region: tectonics controlled by subduction and slab rollback processes. Earth-Science Reviews, 76(3-4), 191-233.

Schumm, S. A. 1985. Patterns of alluvial rivers. Annual Review of Earth and Planetary Sciences, 13, 5.

Stagpoole, V., & Funnell, R. 2001. Arc magmatism and hydrocarbon generation in the northern Taranaki Basin, New Zealand. Petroleum Geoscience, 7(3), 255-267.

Strogen, D. P., Bland, K. J., Nicol, A., & King, P. R. 2014. Paleogeography of the Taranaki Basin region during the latest Eocene–Early Miocene and implications for the 'total drowning'of Zealandia. New Zealand Journal of Geology and Geophysics, 57(2), 110-127.

Strogen, D. P., Higgs, K. E., Griffin, A. G., & Morgans, H. E. 2019. Late Eocene–Early Miocene facies and stratigraphic development, Taranaki Basin, New Zealand: the transition to plate boundary tectonics during regional transgressionDP Strogen et al. Taranaki Basin Oligocene facies development. Geological Magazine, 156(10), 1751-1770.

Uruski, C. and Wood, R., 1991. Structure and stratigraphy of the New Caledonia Basin. Exploration Geophysics, 22(2), pp.411-418.

Uruski, C. and Wood, R., 1991. Structure and stratigraphy of the New Caledonia Basin. Exploration Geophysics, 22(2), pp.411-418.

Uruski, Chris. 2008. Deepwater Taranaki, New Zealand: structural development and petroleum potential. Exploration Geophysics, 39. 10.1071/EG08013.

Wonham, J. P., Jayr, S., Mougamba, R., & Chuilon, P. 2000. 3D sedimentary evolution of a canyon fill (Lower Miocene-age) from the Mandorove Formation, offshore Gabon. Marine and Petroleum Geology, 17(2), 175-197.

Wonham, Jonathan & Jayr, S & Mougamba, R & Chuilon, Pierre. 2000. 3D sedimentary evolution of a canyon fill (Lower Miocene-age) from the Mandorove Formation, offshore Gabon. Marine and Petroleum Geology - MAR PETROL GEOL. 17. 175-197. 10.1016/S0264-8172(99)00033-1.

Wu, W., Li, Q., Yu, J., Lin, C., Li, D., & Yang, T. 2018. The Central Canyon depositional patterns and filling process in east of L ingshui Depression, Q iongdongnan B asin, northern South China Sea. Geological Journal, 53(6), 3064-3081.

Wu, Wei and Li, Quan and Yu, Jing and Lin, Changsong and Li, Dan and Yang, Ting. (2018). The Central Canyon depositional patterns and filling process in east of Lingshui Depression, Qiongdongnan Basin northern South China Sea. Geological Journal. 53. 10.1002/gj.3143.

Yue, Dali and Li, Wei and Wang, Wurong and Hu, Guangyi and Shen, Bingbei and Wang, Wenfeng and Zhang, Manling and Hu, Jiajing. 2019. Analyzing the Architecture of Point Bar of Meandering Fluvial River using Ground Penetratio Radar: A Case Study from Hulun Lake Depression, China. Interpretation. 7. 1-89. 10.1190/int-2018-0144.1.

Zhou, Wei and Wang, Yingmin and Gao, Xianzhi and Zhu, Weilin and Xu, Qiang and Xu, Shang and Cao, Jianzhi and Wu, Jin. (2015). Architecture, evolution history and controlling factors of the Baiyun submarine canyon system from the middle Miocene to Quaternary in the Pearl River Mouth Basin, northern South China Sea. Marine and Petroleum Geology. 67. 10.1016/ j.marpetgeo.2015.05. 015.